Supplement of Atmos. Chem. Phys., 23, 6863–6877, 2023
https://doi.org/10.5194/acp-23-6863-2023-supplement

Atmospheric Chemistry and Physics
Open Access

Supplement of

Saturation vapor pressure characterization of selected low-volatility organic compounds using a residence time chamber

Zijun Li et al.

Correspondence to: Zijun Li (zijun.li@qut.edu.au) and Taina Yli-Juuti (taina.yli-juuti@uef.fi)

Table S1. Density (ρ) for the studied compounds and references for the data.

Groups	Compounds	ρ [g cm^{-3}]	Reference	Reference Temperature [K]
Polyethylene glycol	PEG 6	1180	Krieger et al. (2018)	298
	PEG 7	1206	Krieger et al. (2018)	298
	PEG 8	1234	Krieger et al. (2018)	298
	PEG 9	1257	Extrapolated from the data of PEG3 – 8 in Krieger et al. (2018)	/
Monocarboxylic acid	Palmitic acid	852	Sigma Alrich SDS sheet	298
	Stearic acid	941	CRC Handbook of Chemistry and Physics (2022)	298
Dicarboxylic acid	Azelaic acid	1251	Thalladi et al. (2000)	298
	Sebacic acid	1210	Sigma Alrich SDS sheet	293
Alcohol	meso-Erythritol	1451	CRC Handbook of Chemistry and Physics (2022)	293
	Xylitol	1520	Sigma Alrich SDS sheet	/
Ester	DEHS	912	Topas GmbH product sheet	/

Table S2. Surface tension or energy (σ) for the studied compounds and references for the data.

Groups	Compounds	σ [mN m^{-1}]	Reference	Reference Temperature [K]
Polyethylene glycol	PEG 6	45	Gallaugher (1932)	298
	PEG 7	45	Gallaugher (1932)	298
	PEG 8	45	Gallaugher (1932)	298
	PEG 9	45	Assumed to be the same as PEG6-8	/
Monocarboxylic acid	Palmitic acid	130	Tao and Mcmurry (2002)	298
	Stearic acid	160	Tao and Mcmurry (2002)	298
Dicarboxylic acid	Azelaic acid	180	Bilde et al. (2003)	296
	Sebacic acid	100	Salo et al. (2010)	296
Alcohol	meso-Erythritol	160	Emanuelsson et al. (2016)	298
	Xylitol	160	Assumed to be the same as meso-Erythritol	/
Ester	DEHS	32	Topas GmbH product sheet	/

Table S3. Summary of experimental melting temperatures from literature.

Groups	Compounds	Melting Point (K)		Reference
Polyethylene glycol	PEG6	281.2 ± 1.0		Krieger et al. (2018)
	PEG7	289.2 ± 1.0		Krieger et al. (2018)
	PEG8	297.4 ± 1.0		Krieger et al. (2018)
	PEG9	299		TCI Chemistry product sheet
Monocarboxylic acid [a]	Palmitic acid	min	332.7	Zeng et al. (2009)
		max	336.5	Misra et al. (2007)
	Stearic acid	min	326.1	Eykman (1889)
		max	344.1	Teixeira et al. (2006)
Dicarboxylic acid [a]	Azelaic acid	min	379.7	Khetarpal et al. (1980)
		max	380	Cingolani and Berchiesi (1974)
	Sebacic acid	min	403.9	Roux et al. (2005)
		max	407	Wynberg and Logothetis (1956)
Alcohol [a]	meso-Erythritol	min	381.6	Spaght et al. (2002)
		max	392.2	Jonsdottir et al. (2002)
	Xylitol	min	365.7	Barone et al. (1990)
		max	369	Tong et al. (2007)
Ester	DEHS	225		Topas GmbH product sheet

[a] The minimum and maximum experimental melting temperatures were used in the COSMO*therm* calculations.

Table S4. Summary of experimental heats of fusion used in the COSMO*therm* calculations

Groups	Compounds	Enthalpy of fusion (kJ mol^{-1})		Reference
Monocarboxylic acid	Palmitic acid	min	47	Misra et al. (2007)
		max	54.935	Pacor (1967)
	Stearic acid	min	50.93	Yu et al. (2000)
		max	68.45	Singleton et al. (1950)
Dicarboxylic acid	Azelaic acid	min	29.7	Roux et al. (2005)
		max	35.3	Chen et al. (2009)
	Sebacic acid	min	40.8	Domalski and Hearing (1996)
		max	46.9	Ventolà et al. (2008)
Alcohol	meso-Erythritol	min	38.9	Lopes Jesus et al. (2005)
		max	42.359	Spaght et al. (2002)
	Xylitol	min	33.26	Tong et al. (2007)
		max	37.7	Carpentier et al. (2003)

Table S5. Abbreviations of techniques listed in Tables S6 – S12

Abbreviations	Full Name
ASAP-MS	Atmospheric solids analysis probe mass spectrometry
EDB	Electronic dynamic balance
FT-TDMA	Flow tube–tandem differential mobility analyzer
IVM	Integrated volume method
KE	Knudsen effusion
KEMS	Knudsen effusion mass spectrometer
MOVI-CIMS	Micro-Orifice Volatilization Impactor Coupled to a Chemical Ionization Mass Spectrometer
TDPBMS	Thermal desorption particle beam mass spectrometer
TE	Torsion effusion
TPD-PT-RMS	Temperature-programmed desorption proton-transfer reaction mass spectrometry
V-TDMA	Volatility tandem differential mobility analyzer

Table S6. Summary of measurements of saturation of vapor pressure (p_{sat}) of polyethylene glycols from previous studies.

Study	Compound	$p_{sat, ref}$ (Pa)	T_{ref} (K)	T_{exp} (K)	Techniques	Sample	Uncertainty Type
Krieger et al. (2018)	PEG 6	$3.15^{+0.58}_{-0.49} \times 10^{-5}$	298.15	277 – 323	EDB FT-TDMA KEMS	injected micron droplets atomized, dried aerosols bulk materials	95% CI
	PEG 7	$1.38^{+0.47}_{-0.35} \times 10^{-6}$					
	PEG 8	$9.2^{+20.4}_{-6.4} \times 10^{-8}$					
	PEG 9 (predicted)	$3.7^{+4.1}_{-2.0} \times 10^{-9}$					

Note: T_{ref} is the reference temperature for the reported p_{sat} value; T_{exp} is the experimental temperature; and CI is confidence interval.

Table S7. Summary of measurements of saturation of vapor pressure (p_{sat}) of palmitic acid from previous studies.

Study	$p_{sat,\,ref}$ (Pa)	T_{ref} (K)	T_{exp} (K)	Techniques	Sample	Potential Impact of Solvents	Uncertainty Type
Chattopadhyay and Ziemann (2005)	2.66×10^{-5}	298	298 – 413	TDPBMS	atomized, dried aerosols	YES	NA
Davies and Malpass (1961)	1.91×10^{-5}	298	320 – 333	KE	bulk materials	NO	NA
Tao and Mcmurry (2002)	$1.06^{+0.16}_{-0.16} \times 10^{-5}$	298	283 – 323	V-TDMA	atomized, dried aerosols	YES	NA
Yatavelli and Thornton (2010)	$6.8^{+1.8}_{-1.8} \times 10^{-7}$	298	308 – 363	MOVI-CIMS	homogeneous nucleation	NO	1σ
Cappa et al. (2008)	$1.3^{+0.4}_{-0.4} \times 10^{-7}$ $1.4^{+0.6}_{-0.6} \times 10^{-5}$ (liquid, predicted)	298	NA	TPD-PT-RMS	macroscopic, preheated deposit of atomized, dried aerosols	NO	2σ

Note: T_{ref} is the reference temperature for the reported p_{sat} value; T_{exp} is the experimental temperature; and NA is for not available.

Table S8. Summary of measurements of saturation of vapor pressure (p_{sat}) of stearic acid from previous studies.

Study	$p_{sat,\,ref}$ (Pa)	T_{ref} (K)	T_{exp} (K)	Techniques	Sample	Potential Impact of Solvents	Uncertainty Type
Chattopadhyay and Ziemann (2005)	2.83×10^{-6}	298	298 – 413	TDPBMS	atomized, dried aerosols	YES	NA
Davies and Malpass (1961)	1.38×10^{-6}	298	331 – 340	KE	bulk materials	NO	NA
Tao and Mcmurry (2002)	$5.64^{+0.85}_{-0.85} \times 10^{-7}$	298	283 – 323	V-TDMA	atomized, dried aerosols	YES	NA
Cappa et al. (2008)	$9.5^{+3.5}_{-3.5} \times 10^{-8}$ $2.2^{+1.1}_{-1.1} \times 10^{-6}$ (liquid, predicted)	298	NA	TPD-PT-RMS	macroscopic, preheated deposit of atomized, dried aerosols	NO	2σ

Note: T_{ref} is the reference temperature for the reported p_{sat} value; T_{exp} is the experimental temperature; and NA is for not available.

Table S9. Summary of measurements of saturation of vapor pressure (p_{sat}) of azelaic acid from previous studies.

Study	$p_{sat,\,ref}$ (Pa)	T_{ref} (K)	T_{exp} (K)	Techniques	Sample	Potential Impact of Solvents	Uncertainty Type
Salo et al. (2010)	$4.7^{+0.8}_{-0.8} \times 10^{-5}$	298	298 – 573	V-TDMA	atomized, dried aerosols	YES	95% CI
Oxford et al. (2019)	2.2×10^{-5}	298	293 – 314	V-TDMA	atomized, dried aerosols	YES	NA
Saleh et al. (2010)	$1.4^{+0.5}_{-0.5} \times 10^{-5}$ (A) $9.0^{+3.0}_{-3.0} \times 10^{-6}$ (B)	298	297 – 320	IVM	atomized, dried aerosols (a) homogeneous nucleation (b)	YES NO	95% CI
Bilde et al. (2003)	$9.4^{+4.7}_{-4.7} \times 10^{-6}$	298	372 – 401	FT-TDMA	atomized, dried aerosols	YES	total relative uncertainty
Chattopadhyay and Ziemann (2005)	7.41×10^{-6}	298	298 – 413	TDPBMS	atomized, dried aerosols	YES	NA
Bilde et al. (2015)	$1.7^{+2.7}_{-1.0} \times 10^{-5}$	298	n/a	n/a	n/a	n/a	95% CI
Ribeiro da Silva et al. (1999)	$6.3^{+5.0}_{-5.0} \times 10^{-7}$	298	367 – 377	KE	bulk materials	NO	NA
Yatavelli and Thornton (2010)	$7.0^{+2.8}_{-2.8} \times 10^{-8}$	298	308 – 363	MOVI-CIMS	homogeneous nucleation	NO	1σ
Bruns et al. (2012)	$6.9^{+4.2}_{-4.2} \times 10^{-8}$	298	337 – 372	ASAP-MS	remaining sample after evaporation of solvent	NO	95% CI
Cappa et al. (2007)	$1.0^{+0.6}_{-0.6} \times 10^{-8}$	298	348 -373	TPD-PT-RMS	macroscopic, preheated deposit of atomized, dried aerosols	NO	2σ

Note: T_{ref} is the reference temperature for the reported p_{sat} value; T_{exp} is the experimental temperature; CI is confidence interval; NA is for not available; and n/a is not applicable.

Table S10. Summary of measurements of saturation of vapor pressure (p_{sat}) of sebacic acid from previous studies.

Study	$p_{sat,\,ref}$ (Pa)	T_{ref} (K)	T_{exp} (K)	Techniques	Sample	Potential Impact of Solvents	Uncertainty Type
Salo et al. (2010)	$9.0^{+5.0}_{-5.0} \times 10^{-6}$	298	298 – 573	V-TDMA	atomized, dried aerosols	YES	95% CI
Chattopadhyay and Ziemann (2005)	1.47×10^{-6}	298	298 – 413	TDPBMS	atomized, dried aerosols	YES	NA
Bilde et al. (2015)	$4.8^{+11.5}_{-3.4} \times 10^{-7}$	298	n/a	n/a	n/a	n/a	95% CI
Bruns et al. (2012)	$7.8^{+3.2}_{-3.2} \times 10^{-8}$	298	337 – 389	ASAP-MS	remaining sample after evaporation of solvent	NO	95% CI
Davies and Thomas (1960)	7.6×10^{-8}	298	375 – 403	KE	bulk materials	NO	NA
Cappa et al. (2007)	$1.6^{+0.8}_{-0.8} \times 10^{-8}$	298	353 – 385	TPD-PT-RMS	macroscopic, preheated deposit of atomized, dried aerosols	NO	2σ

Note: T_{ref} is the reference temperature for the reported p_{sat} value; T_{exp} is the experimental temperature; CI is confidence interval; NA is for not available; and n/a is not applicable.

Table S11. Summary of measurements of saturation of vapor pressure (p_{sat}) of dioctyl sebacate (DOS) from previous studies.

Study	$p_{sat, ref}$ (Pa)	T_{ref} (K)	T_{exp} (K)	Techniques	Sample	Uncertainty Type
Rader et al. (1987)	2.74×10^{-6}	298	298	FT-TDMA	atomized, dried aerosols	NA

Note: T_{ref} is the reference temperature for the reported p_{sat} value; T_{exp} is the experimental temperature; and NA is for not available.

Table S12. Summary of measurements of saturation of vapor pressure (p_{sat}) of meso-erythritol and xylitol from previous studies.

Study	$p_{sat, ref}$ (Pa)	T_{ref} (K)	T_{exp} (K)	Techniques	Sample	Uncertainty Type
			meso-erythritol			
Barone et al. (1990)	$2.5^{+3.1}_{-1.4} \times 10^{-5}$ (liquid)	298	397 – 428	TE	bulk materials	2σ
Emanuelsson et al. (2016)	$6.3^{+3.1}_{-3.1} \times 10^{-5}$ (liquid) $2.8^{+1.4}_{-1.4} \times 10^{-5}$ (crystalline solid)	298	298, 303, 308	FT-TDMA	atomized, dried aerosols	1σ
			xylitol			
Barone et al. (1990)	$4.7^{+4.3}_{-2.6} \times 10^{-6}$ (liquid)	298	406 – 460	TE	bulk materials	2σ

Note: T_{ref} is the reference temperature for the reported p_{sat} value; and T_{exp} is the experimental temperature

Table S13. Saturation vapor pressures calculated with COSMO*therm* using two different conformer sets.

Groups	Compounds	COSMO*base* [a]	0 H-bonds [b]
Polyethylene glycol	PEG 6	5.42×10^{-10}	9.56×10^{-9}
	PEG 7	1.59×10^{-9}	8.83×10^{-8}
	PEG 8	3.76×10^{-13}	1.10×10^{-12}
	PEG 9	1.72×10^{-15}	4.10×10^{-12}
Monocarboxylic acid	Palmitic acid	$(1.14 - 2.06) \times 10^{-5}$	n/a
	Stearic acid	$(0.51 - 3.76) \times 10^{-6}$	n/a
Dicarboxylic acid	Azelaic acid	$(1.36 - 2.29) \times 10^{-6}$	$(2.44 - 4.10) \times 10^{-6}$
	Sebacic acid	$(1.95 - 4.24) \times 10^{-9}$	$(0.98 - 2.14) \times 10^{-7}$
Alcohol	meso-Erythritol	$(0.69 - 1.37) \times 10^{-5}$	$(1.57 - 3.10) \times 10^{-5}$
	Xylitol	$(2.28 - 3.62) \times 10^{-6}$	$(3.55 - 5.63) \times 10^{-8}$
Ester	DEHS	9.23×10^{-7}	n/a

[a] Conformers from COSMO*base* (azelaic acid, sebacic acid, palmitic acid, stearic acid, meso-erythritol and xylitol) or computed using the BP-TZVPD-FINE-COSMO+GAS_18.xml template of COSMO*conf* (DEHS, PEG6 – 9). [b] Conformers containing no intramolecular H-bonds from systematic conformer sampling described by (Kurtén et al., 2018). Note: n/a is not applicable.

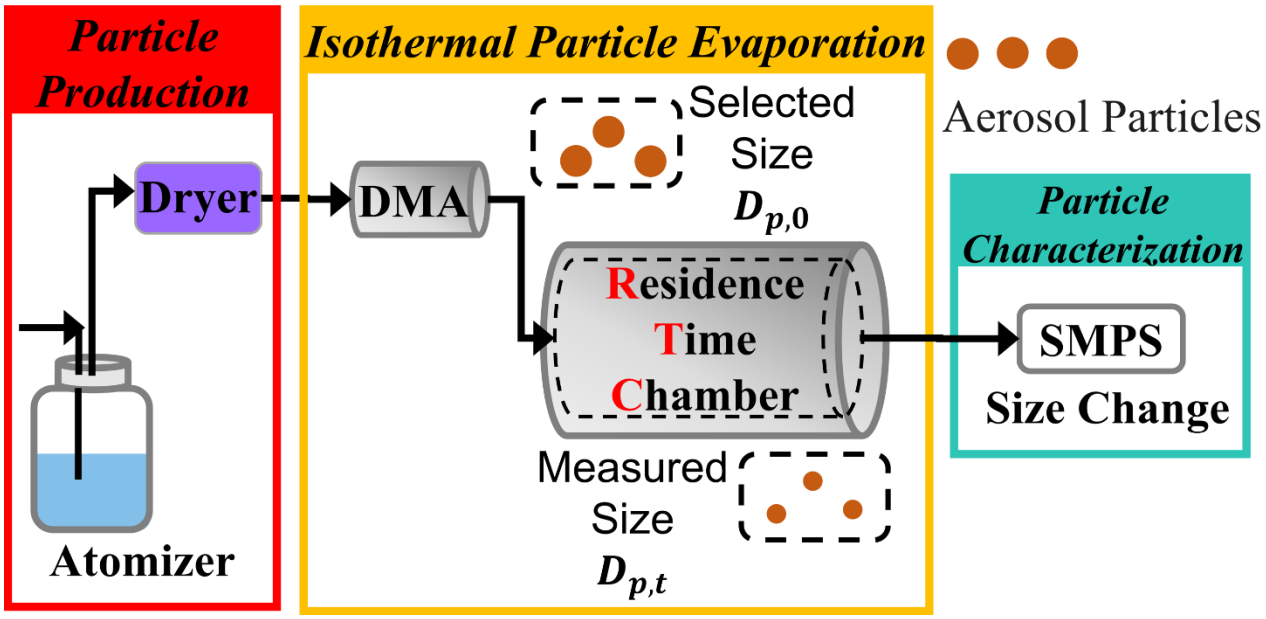

Figure S1. Schematic diagram of the measurement setup for isothermal particle evaporation.

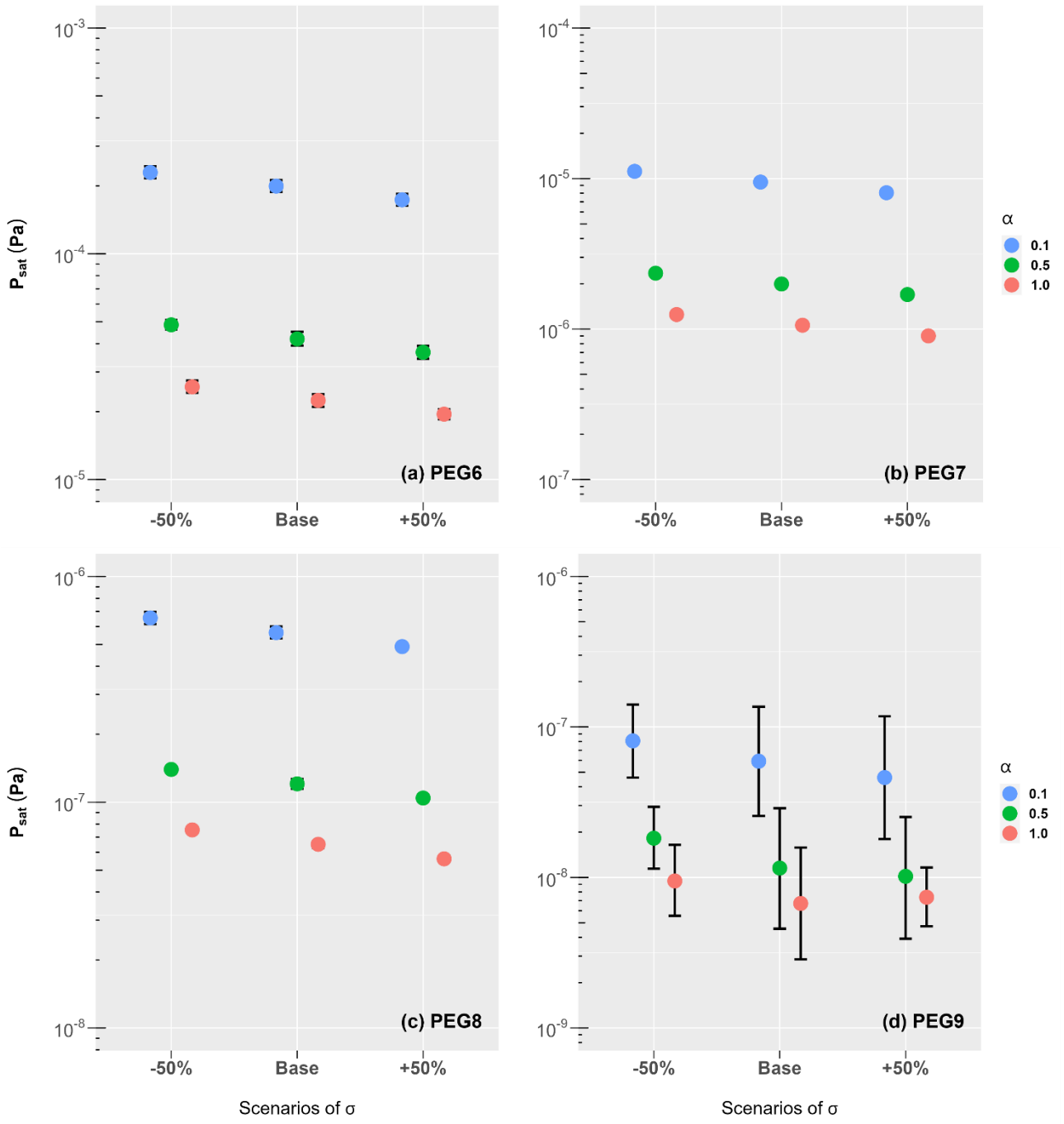

Figure S2. Sensitivity analyses with different combinations of accommodation coefficient (α) (1.0, red; 0.5, green; 0.1, blue) and surface tension/energy (σ) (-50%, Base, +50%) for PEGs (PEG 6 – 9). The base case of σ is the reference condition, representing those σ values shown in Table 1 in the main text. The error bars stand for the 95% credible intervals.

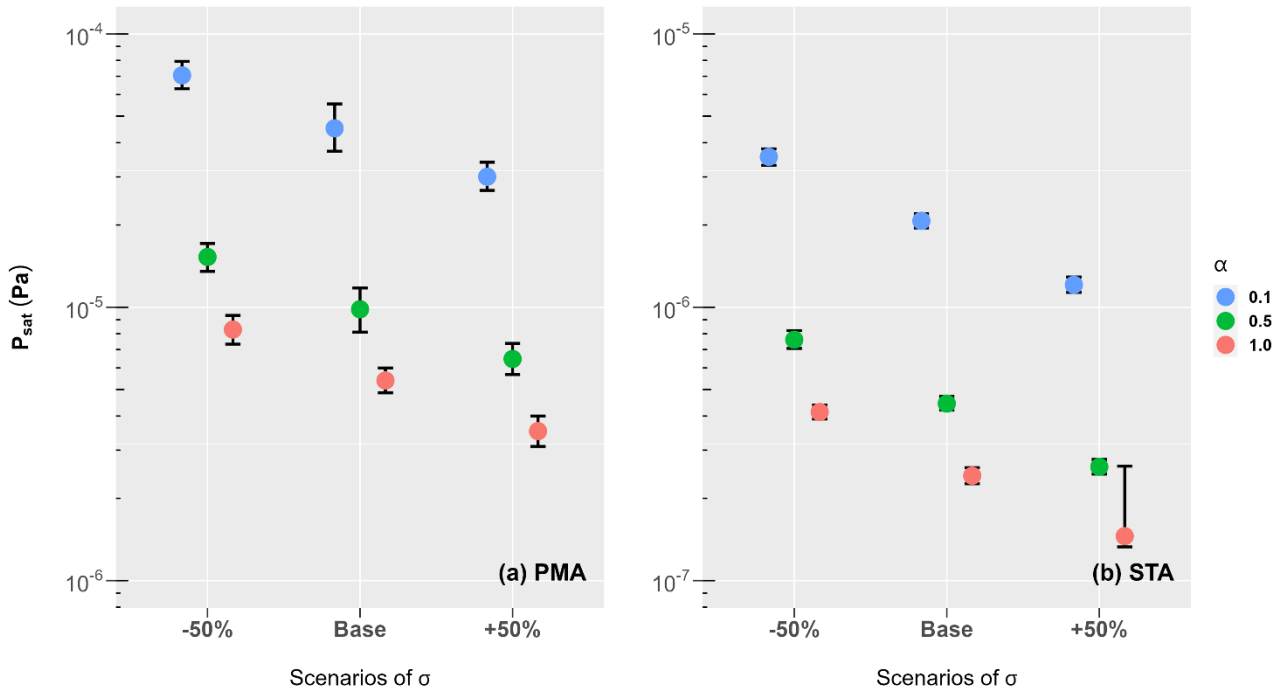

Figure S3. Sensitivity analyses with different combinations of accommodation coefficient (α) (1.0, red; 0.5, green; 0.1, blue) and surface tension/energy (σ) (-50%, Base, +50%) for palmitic acid (PMA, a) and stearic acid (STA, b). The base case of σ is the reference condition, representing those σ values shown in Table 1 in the main text. The error bars stand for the 95% credible intervals.

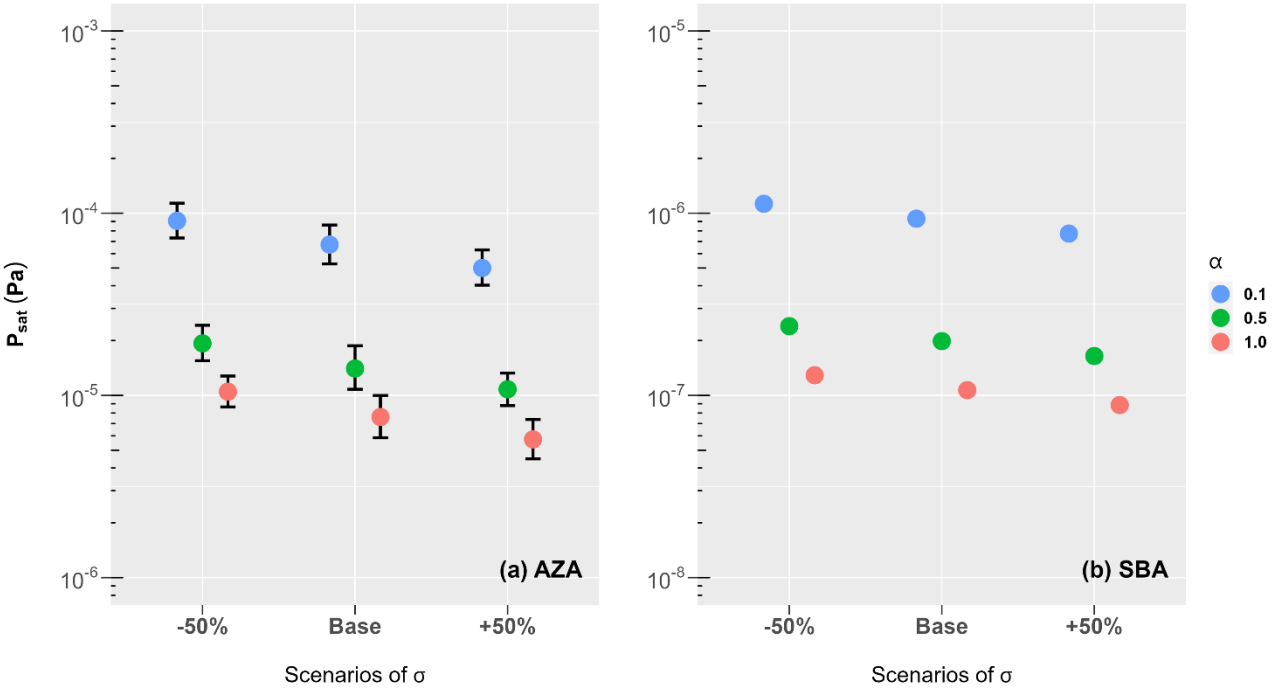

Figure S4. Sensitivity analyses with different combinations of accommodation coefficient (α) (1.0, red; 0.5, green; 0.1, blue) and surface tension/energy (σ) (-50%, Base, +50%) for azelaic acid (AZA, a) and sebacic acid (SBA, b). The base case of σ is the reference condition, representing those σ values shown in Table 1 in the main text. The error bars stand for the 95% credible intervals.

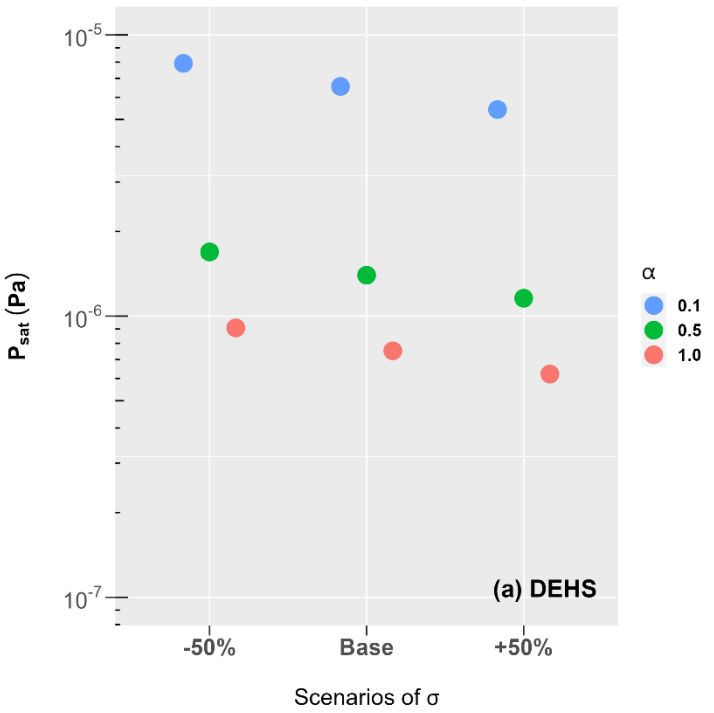

Figure S5. Sensitivity analyses with different combinations of accommodation coefficient (α) (1.0, red; 0.5, green; 0.1, blue) and surface tension/energy (σ) (-50%, Base, +50%) for di-2-ethylhexyl sebacate (DEHS). The base case of σ is the reference condition, representing the σ value shown in Table 1 in the main text. The error bars stand for the 95% credible intervals.

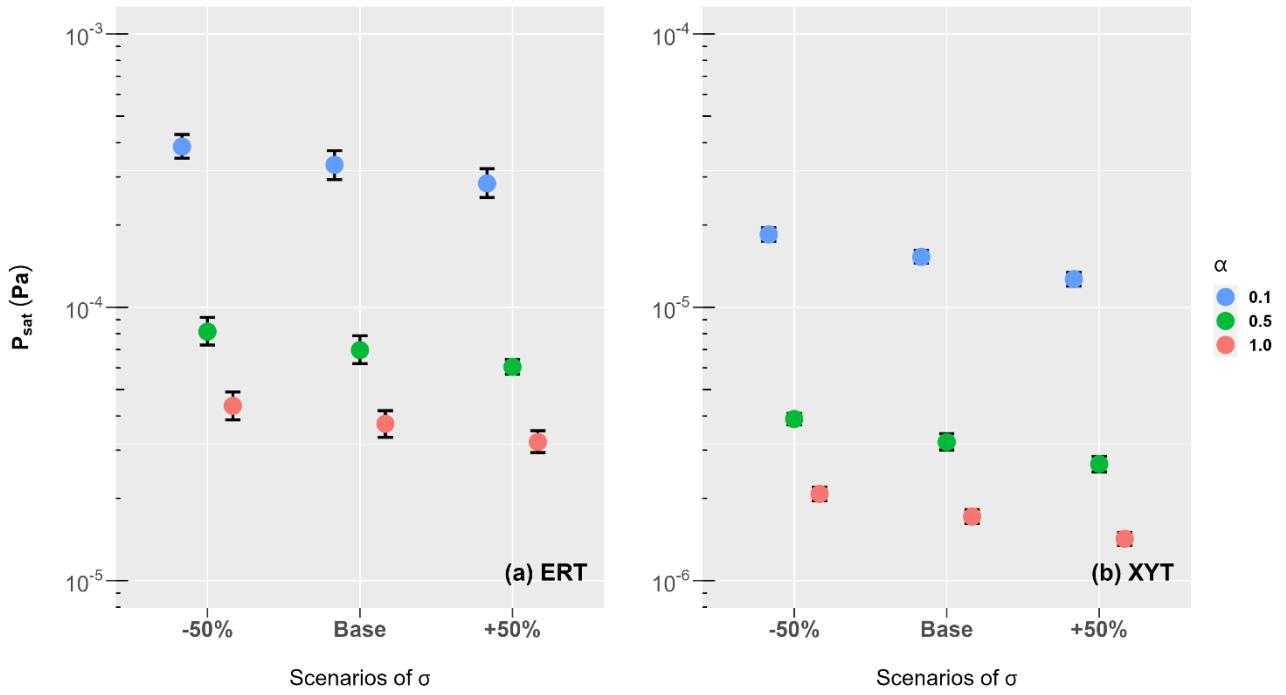

Figure S6. Sensitivity analyses with different combinations of accommodation coefficient (α) (1.0, red; 0.5, green; 0.1, blue) and surface tension/energy (σ) (-50%, Base, +50%) for meso-erythritol (ERT, a) and xylitol (XYT, b). The base case of σ is the reference condition, representing those σ values shown in Table 1 in the main text. The error bars stand for the 95% credible intervals.

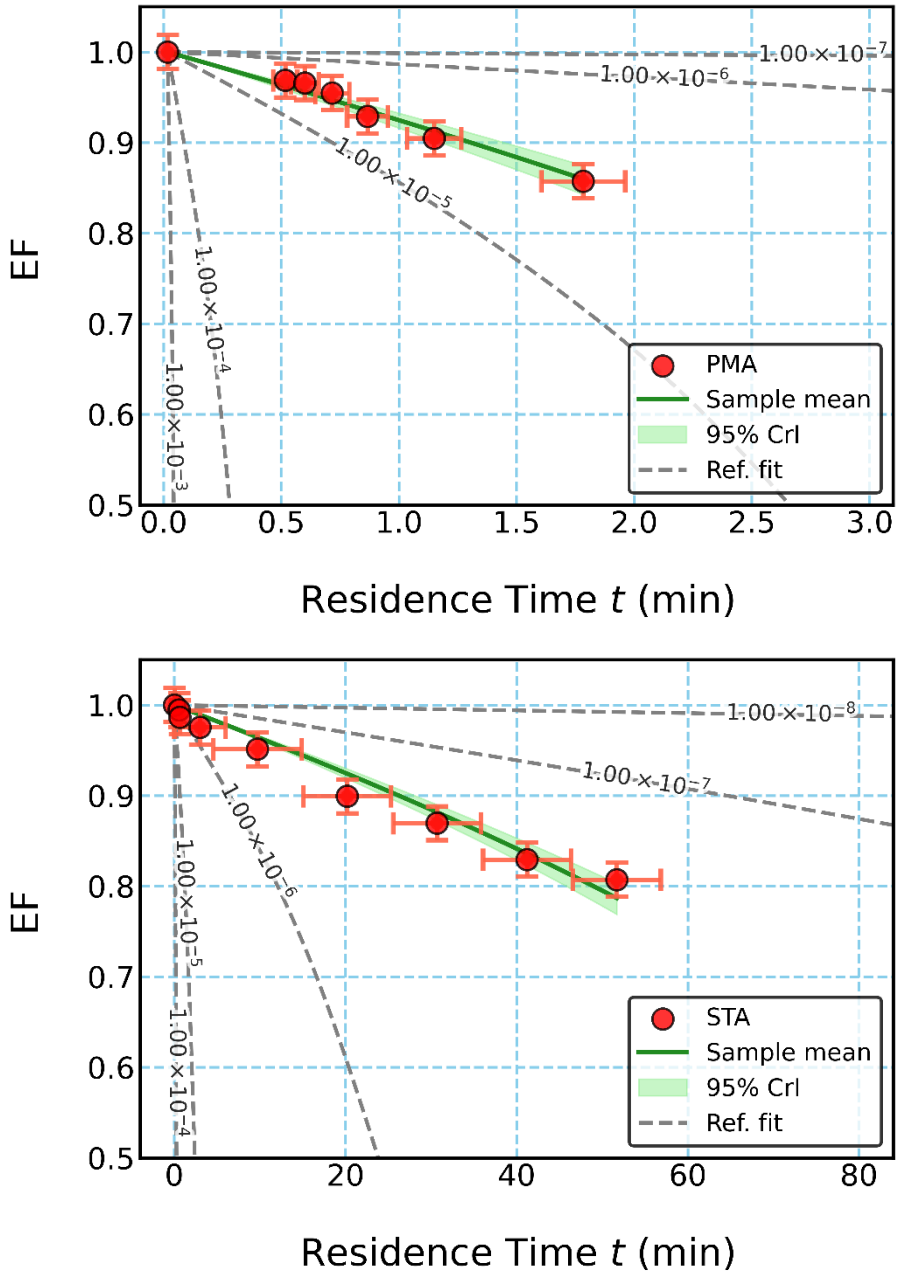

Figure S7. Measured evaporation factors (EFs; circles) as a function of residence time for palmitic acid (PMA) and stearic acid (STA), simulations with average optimized p_{sat} values (solid lines; green) and 95% credible intervals (95% CrIs; shaded areas in green) with the optimized p_{sat} values, and simulated evaporation curves with a set of reference p_{sat} values (10^{-8} to 10^{-3} Pa, with one-decade intervals, dashed grey lines). All the simulated evaporation curves were computed using α = 1 and the chosen σ shown in Table 1 in the main text. For the measured data points of EF, the error bars represent the maximum uncertainty of ±1.875% in particle size measurements on y-axis and the minimum and maximum residence times on x-axis.

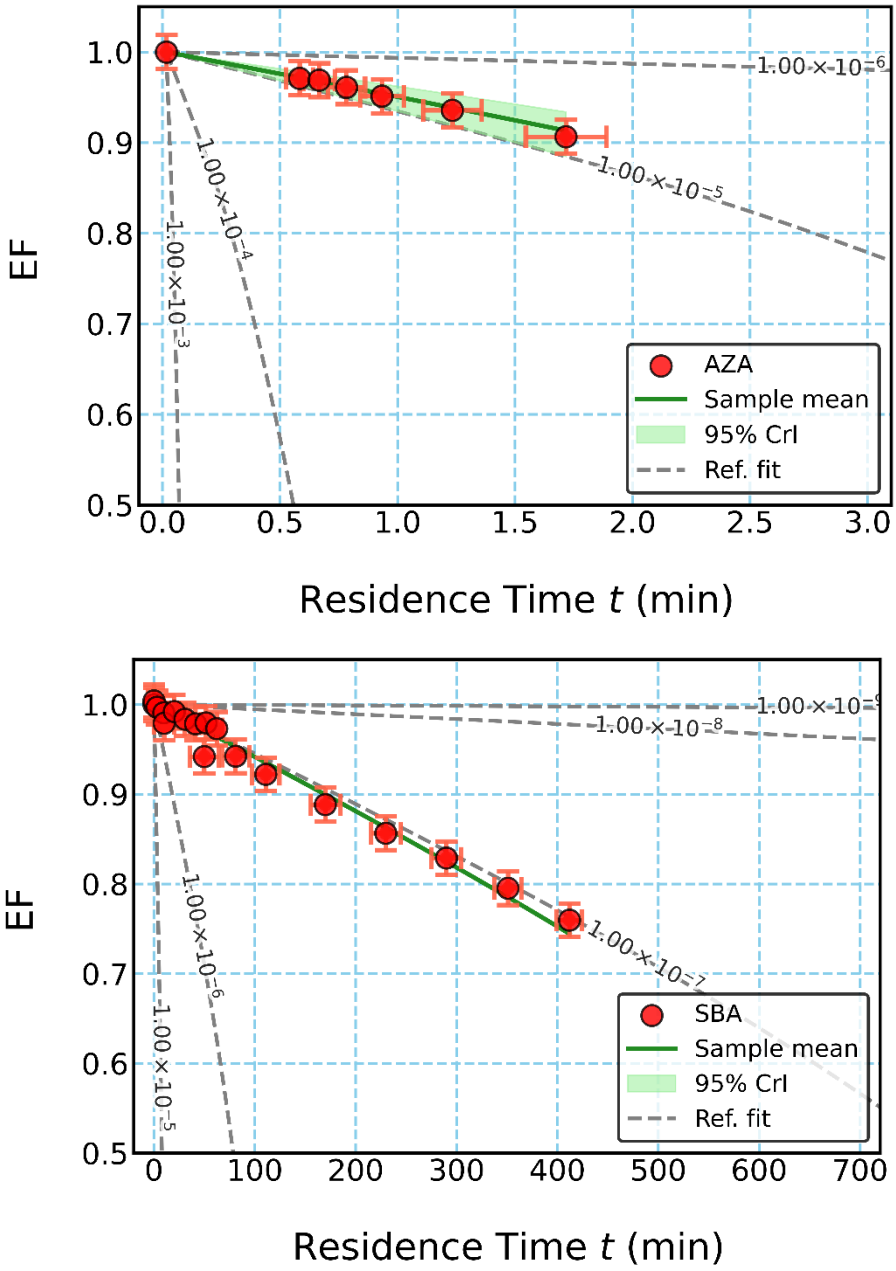

Figure S8. Measured evaporation factors (EFs; circles) as a function of residence time for azelaic acid (AZA) and sebacic acid (SBA), simulations with average optimized p_{sat} values (solid lines; green) and 95% credible intervals (95% CrIs; shaded areas in green) with the optimized p_{sat} values, and simulated evaporation curves with a set of reference p_{sat} values (10^{-9} to 10^{-3} Pa, with one-decade intervals, dashed grey lines). All the simulated evaporation curves were computed using α = 1 and the chosen σ shown in Table 1 in the main text. For the measured data points of EF, the error bars represent the maximum uncertainty of ±1.875% in particle size measurements on y-axis and the minimum and maximum residence times on x-axis.

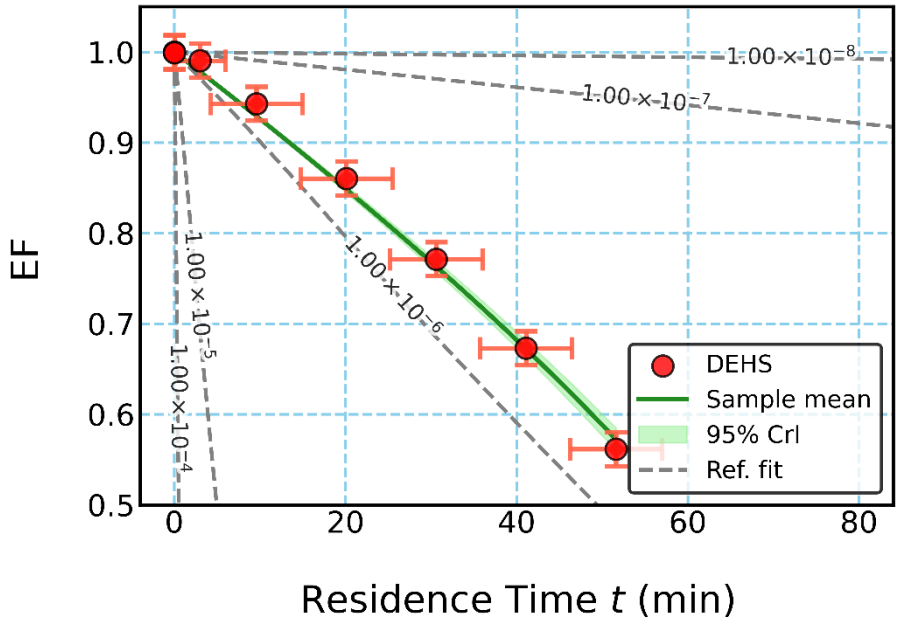

Figure S9. Measured evaporation factors (EFs; circles) as a function of residence time for di-2-ethylhexyl sebacate (DEHS), simulations with average optimized p_{sat} value (solid line; green) and 95% credible interval (95% CrI; shaded areas in green) with the optimized p_{sat} values, and simulated evaporation curves with a set of reference p_{sat} values (10^{-8} to 10^{-4} Pa, with one-decade intervals, dashed grey lines). All the simulated evaporation curves were computed using α = 1 and the chosen σ shown in Table 1 in the main text. For the measured data points of EF, the error bars represent the maximum uncertainty of ±1.875% in particle size measurements on y-axis and the minimum and maximum residence times on x-axis.

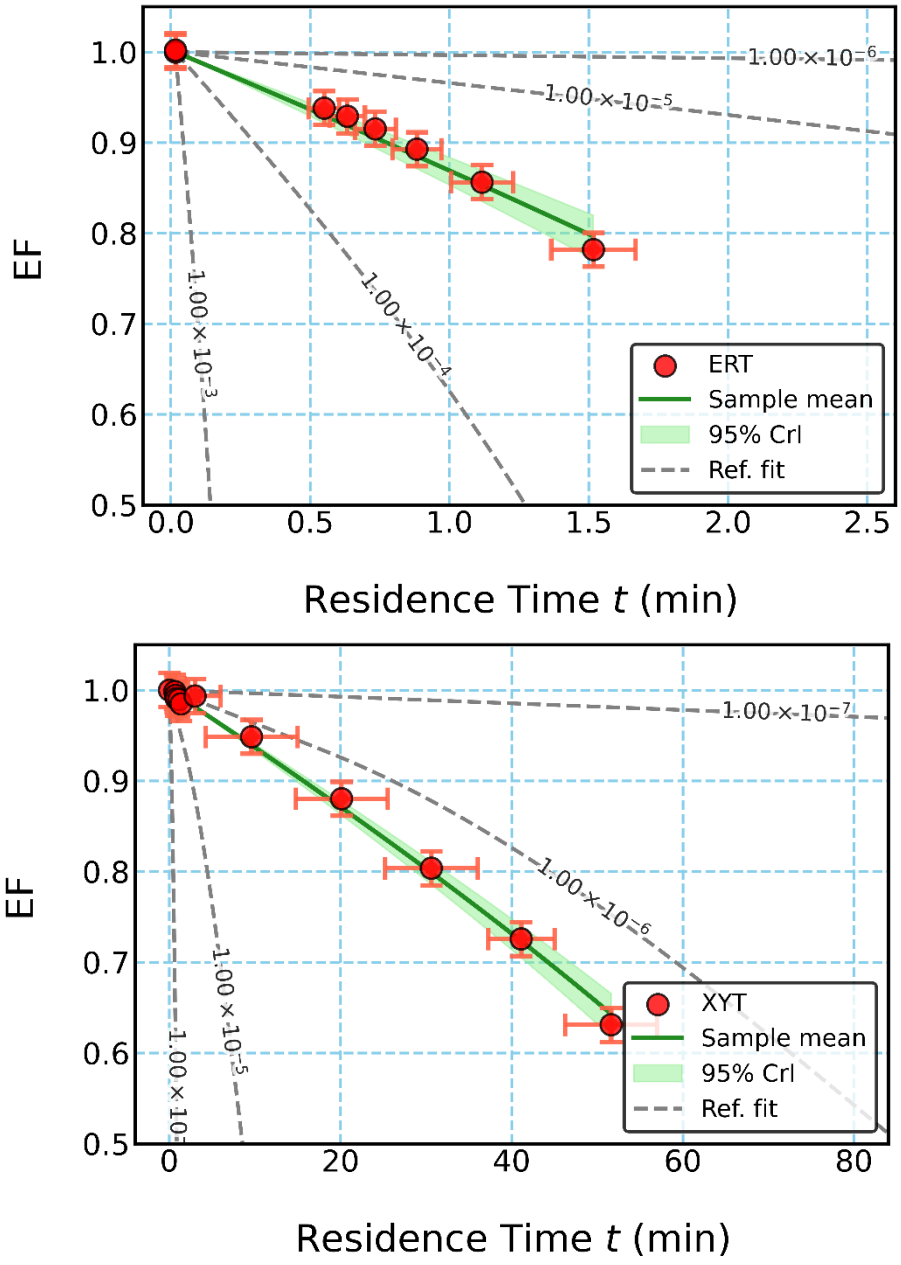

Figure S10. Measured evaporation factors (EFs; circles) as a function of residence time for meso-erythritol (ERT) and xylitol (XYT), simulations with average optimized p_{sat} values (solid lines; green) and 95% credible intervals (95% CrIs; shaded areas in green) with the optimized p_{sat} values, and simulated evaporation curves with a set of reference p_{sat} values (10^{-7} to 10^{-3} Pa, with one-decade intervals, dashed grey lines). All the simulated evaporation curves were computed using α = 1 and the chosen σ shown in Table 1 in the main text. For the measured data points of EF, the error bars represent the maximum uncertainty of ±1.875% in particle size measurements on y-axis and the minimum and maximum residence times on x-axis.

References

Barone, G., Gatta, G. D., Ferro, D., and Piacente, V.: Enthalpies and entropies of sublimation, vaporization and fusion of nine polyhydric alcohols, Journal of the Chemical Society, Faraday Transactions, 86, 75-79, 10.1039/ft9908600075, 1990.

Bilde, M., Svenningsson, B., Mønster, J., and Rosenørn, T.: Even−odd alternation of evaporation rates and vapor pressures of C_3−C_9 dicarboxylic acid aerosols, Environmental Science & Technology, 37, 1371-1378, 10.1021/es0201810, 2003.

Bilde, M., Barsanti, K., Booth, M., Cappa, C. D., Donahue, N. M., Emanuelsson, E. U., McFiggans, G., Krieger, U. K., Marcolli, C., Topping, D., Ziemann, P., Barley, M., Clegg, S., Dennis-Smither, B., Hallquist, M., Hallquist, A. M., Khlystov, A., Kulmala, M., Mogensen, D., Percival, C. J., Pope, F., Reid, J. P., Ribeiro da Silva, M. A., Rosenoern, T., Salo, K., Soonsin, V. P., Yli-Juuti, T., Prisle, N. L., Pagels, J., Rarey, J., Zardini, A. A., and Riipinen, I.: Saturation vapor pressures and transition enthalpies of low-volatility organic molecules of atmospheric relevance: From dicarboxylic acids to complex mixtures, Chem Rev, 115, 4115-4156, 10.1021/cr5005502, 2015.

Bruns, E. A., Greaves, J., and Finlayson-Pitts, B. J.: Measurement of vapor pressures and heats of sublimation of dicarboxylic acids using atmospheric solids analysis probe mass spectrometry, J Phys Chem A, 116, 5900-5909, 10.1021/jp210021f, 2012.

Cappa, C. D., Lovejoy, E. R., and Ravishankara, A. R.: Determination of evaporation rates and vapor pressures of very low volatility compounds: A study of the C_4-C_{10} and C_{12} dicarboxylic acids, J Phys Chem A, 111, 3099-3109, 10.1021/jp068686q, 2007.

Cappa, C. D., Lovejoy, E. R., and Ravishankara, A. R.: Evaporation rates and vapor pressures of the even-numbered C_8-C_{18} monocarboxylic acids, J Phys Chem A, 112, 3959-3964, 10.1021/jp710586m, 2008.

Carpentier, L., Desprez, S., and Descamps, M.: Crystallization and glass properties of pentitols, Journal of Thermal Analysis and Calorimetry, 73, 577-586, 10.1023/a:1025482230325, 2003.

Chattopadhyay, S. and Ziemann, P. J.: Vapor pressures of substituted and unsubstituted monocarboxylic and dicarboxylic acids measured using an improved thermal desorption particle beam mass spectrometry method, Aerosol Science and Technology, 39, 1085-1100, 10.1080/02786820500421547, 2005.

Chen, S.-n., Xia, Q., Li, D., Yuan, W.-G., Zhang, F.-B., and Zhang, G.-L.: Solid−liquid equilibria of nonanedioic acid in binary ethanol + water solvent mixtures from (292.35 to 345.52) K, Journal of Chemical & Engineering Data, 54, 1395-1399, 10.1021/je800921n, 2009.

Cingolani, A. and Berchiesi, G.: Thermodynamic properties of organic compounds, Journal of thermal analysis, 6, 87-90, 10.1007/BF01911490, 1974.

CRC Handbook of Chemistry and Physics: CRC handbook of chemistry and physics, 103rd edition, 2022.

Davies, M. and Malpass, V. E.: 212. Heats of sublimation of straight-chain monocarboxylic acids, Journal of the Chemical Society (Resumed), 1048-1055, 10.1039/jr9610001048, 1961.

Davies, M. and Thomas, G. H.: The lattice energies, infra-red spectra, and possible cyclization of some dicarboxylic acids, Transactions of the Faraday Society, 56, 185-192, 10.1039/tf9605600185, 1960.

Domalski, E. S. and Hearing, E. D.: Heat capacities and entropies of organic compounds in the condensed phase. Volume III, Journal of Physical and Chemical Reference Data, 25, 1-525, 10.1063/1.555985, 1996.

Emanuelsson, E. U., Tschiskale, M., and Bilde, M.: Phase state and saturation vapor pressure of submicron particles of meso-erythritol at ambient conditions, J Phys Chem A, 120, 7183-7191, 10.1021/acs.jpca.6b04349, 2016.

Eykman, J. F.: Zur kryoskopischen molekulargewichtsbestimung, Zeitschrift für Physikalische Chemie, 4U, 497-519, 10.1515/zpch-1889-0436, 1889.

Gallaugher, A. F.: The physical and chemical properties of the polyethylene glycols and their derivatives, 1932.

Jonsdottir, S. O., Cooke, S. A., and Macedo, E. A.: Modeling and measurements of solid-liquid and vapor-liquid equilibria of polyols and carbohydrates in aqueous solution, Carbohydr Res, 337, 1563-1571, 10.1016/s0008-6215(02)00213-6, 2002.

Khetarpal, S., Lal, K., and Bhatnagar, H. L.: Melt viscosities of succinic, glutaric, adipic, pimelic, suberic, azelaic & sebacic acids, 1980.

Krieger, U. K., Siegrist, F., Marcolli, C., Emanuelsson, E. U., Gøbel, F. M., Bilde, M., Marsh, A., Reid, J. P., Huisman, A. J., Riipinen, I., Hyttinen, N., Myllys, N., Kurtén, T., Bannan, T., Percival, C. J., and Topping, D.: A reference data set for validating vapor pressure measurement techniques: Homologous series of polyethylene glycols, Atmospheric Measurement Techniques, 11, 49-63, 10.5194/amt-11-49-2018, 2018.

Kurtén, T., Hyttinen, N., D'Ambro, E. L., Thornton, J., and Prisle, N. L.: Estimating the saturation vapor pressures of isoprene oxidation products $C_5H_{12}O_6$ and $C_5H_{10}O_6$ using COSMO-RS, Atmospheric Chemistry and Physics, 18, 17589-17600, 10.5194/acp-18-17589-2018, 2018.

Lopes Jesus, A. J., Tome, L. I., Eusebio, M. E., and Redinha, J. S.: Enthalpy of sublimation in the study of the solid state of organic compounds. Application to erythritol and threitol, J Phys Chem B, 109, 18055-18060, 10.1021/jp051621n, 2005.

Misra, A. K., Misra, M., Panpalia, G. M., and Dorle, A. K.: Thermoanalytical and microscopic investigation of interaction between paracetamol and fatty acid crystals, Journal of Macromolecular Science, Part A, 44, 685-690, 10.1080/10601320701351177, 2007.

Oxford, C. R., Rapp, C. M., Wang, Y., Kumar, P., Watson, D., Portelli, J. L., Sussman, E. A., Dhawan, S., Jiang, J., and Williams, B. J.: Development and qualification of a VH-TDMA for the study of pure aerosols, Aerosol Science and Technology, 53, 120-132, 10.1080/02786826.2018.1547358, 2019.

Pacor, P.: Applicability of the du pont 900 dta apparatus in quantitative differential thermal analysis, Analytica Chimica Acta, 37, 200-208, 10.1016/s0003-2670(01)80660-7, 1967.

Rader, D. J., McMurry, P. H., and Smith, S.: Evaporation rates of monodisperse organic aerosols in the 0.02- to 0.2-μm-diameter range, Aerosol Science and Technology, 6, 247-260, 10.1080/02786828708959137, 1987.

Ribeiro da Silva, M. A. V., Monte, M. J. S., and Ribeiro, J. R.: Vapour pressures and the enthalpies and entropies of sublimation of five dicarboxylic acids, The Journal of Chemical Thermodynamics, 31, 1093-1107, 10.1006/jcht.1999.0522, 1999.

Roux, M. V., Temprado, M., and Chickos, J. S.: Vaporization, fusion and sublimation enthalpies of the dicarboxylic acids from C_4 to C_{14} and C_{16}, The Journal of Chemical Thermodynamics, 37, 941-953, 10.1016/j.jct.2004.12.011, 2005.

Saleh, R., Khlystov, A., and Shihadeh, A.: Effect of aerosol generation method on measured saturation pressure and enthalpy of vaporization for dicarboxylic acid aerosols, Aerosol Science and Technology, 44, 302-307, 10.1080/02786821003591810, 2010.

Salo, K., Jonsson, A. M., Andersson, P. U., and Hallquist, M.: Aerosol volatility and enthalpy of sublimation of carboxylic acids, J Phys Chem A, 114, 4586-4594, 10.1021/jp910105h, 2010.

Singleton, W. S., Ward, T. L., and Dollear, F. G.: Physical properties of fatty acids. I. Some dilatometric and thermal properties of stearic acid in two polymorphic forms, Journal of the American Oil Chemists Society, 27, 143-146, 10.1007/bf02634385, 1950.

Spaght, M. E., Thomas, S. B., and Parks, G. S.: Some heat-capacity data on organic compounds obtained with a radiation calorimeter, The Journal of Physical Chemistry, 36, 882-888, 10.1021/j150333a009, 2002.

Tao, Y. and McMurry, P. H.: Vapor pressures and surface free energies of C_{14}-C_{18} monocarboxylic acids and C_5 and C_6 dicarboxylic acids, Environmental Science & Technology, 23, 1519-1523, 10.1021/es00070a011, 2002.

Teixeira, A. C., Goncalves da Silva, A. M., and Fernandes, A. C.: Phase behaviour of stearic acid-stearonitrile mixtures. A thermodynamic study in bulk and at the air-water interface, Chem Phys Lipids, 144, 160-171, 10.1016/j.chemphyslip.2006.09.001, 2006.

Thalladi, V. R., Nüsse, M., and Boese, R.: The melting point alternation in α, ω-alkanedicarboxylic acids, Journal of the American Chemical Society, 122, 9227-9236, 10.1021/ja0011459, 2000.

Tong, B., Tan, Z.-C., Shi, Q., Li, Y.-S., Yue, D.-T., and Wang, S.-X.: Thermodynamic investigation of several natural polyols (I): Heat capacities and thermodynamic properties of xylitol, Thermochimica Acta, 457, 20-26, 10.1016/j.tca.2007.02.022, 2007.

Ventolà, L., Bayés, L., Benages, R., Novegil-Anleo, F. J., Cuevas-Diarte, M. Á., Calvet, T., and Mondieig, D.: Decanedioic acid ($C_{10}H_{18}O_4$)/dodecanedioic acid ($C_{12}H_{22}O_4$) system: Polymorphism of the components and experimental phase diagram, Helvetica Chimica Acta, 91, 1286-1298, 10.1002/hlca.200890140, 2008.

Wynberg, H. and Logothetis, A.: Studies in the synthesis of long-chain compounds[1, 2], Journal of the American Chemical Society, 78, 1958-1961, doi.org/10.1021/ja01590a054, 1956.

Yatavelli, R. L. N. and Thornton, J. A.: Particulate organic matter detection using a micro-orifice volatilization impactor coupled to a chemical ionization mass spectrometer (MOVI-CIMS), Aerosol Science and Technology, 44, 61-74, 10.1080/02786820903380233, 2010.

Yu, S., Meng, S., Tan, Z., Li, L., and Zhang, J.: Heat capacity and thermodynamic properties of stearic acid, Acta Energiae Solaris Sinica, 21, 171-175, 2000.

Zeng, J. L., Cao, Z., Yang, D. W., Xu, F., Sun, L. X., Zhang, L., and Zhang, X. F.: Phase diagram of palmitic acid-tetradecanol mixtures obtained by dsc experiments, Journal of Thermal Analysis and Calorimetry, 95, 501-505, 10.1007/s10973-008-9274-x, 2009.